

**Stanislav Myslenkov<sup>1,2,3\*</sup>, Alisa Medvedeva<sup>2</sup>, Victor Arkhipkin<sup>1</sup>, Margarita Markina<sup>1,2</sup>, Galina Surkova<sup>1</sup>, Aleksey Krylov<sup>1</sup>, Sergey Dobrolyubov<sup>1</sup>, Sergey Zilitinkevich<sup>1,4</sup>, Peter Koltermann<sup>1</sup>**

<sup>1</sup> Lomonosov Moscow State University, Moscow, Russia

<sup>2</sup> P.P. Shirshov Institute of Oceanology, Russian Academy of Sciences, Moscow, Russia

<sup>3</sup> Hydrometeorological Research Centre of the Russian Federation, Marine forecast division

<sup>4</sup> Finnish Meteorological Institute, Helsinki, Finland

\* **Corresponding author:** stasocean@gmail.com

# LONG-TERM STATISTICS OF STORMS IN THE BALTIC, BARENTS AND WHITE SEAS AND THEIR FUTURE CLIMATE PROJECTIONS

**ABSTRACT.** The numerical model simulations of storm activity in the White, Baltic and Barents Seas were analyzed for the period from 1979 to 2015. In this paper the storm number of these seas was calculated. The connections of wind wave climate with indices of large-scale atmospheric circulation such as NAO, AO and SCAND were estimated. Also, the future changes of wind wave climate were analysed.

**KEY WORDS:** wind waves, storm, climate change, SWAN, reanalysis, Baltic Sea, Barents Sea, White Sea, significant wave height, trend, storminess, model, future change, NAO, AO, SCAND, large-scale atmospheric circulation

**CITATION:** Stanislav Myslenkov, Alisa Medvedeva, Victor Arkhipkin, Margarita Markina, Galina Surkova, Aleksey Krylov, Sergey Dobrolyubov, Sergey Zilitinkevich, Peter Koltermann (2018) Long-term Statistics of Storms in the Baltic, Barents and White Seas and Their Future Climate Projections. *Geography, Environment, Sustainability*, Vol.11, No 1, p. 93-112

DOI-10.24057/2071-9388-2018-11-1-93-112

## INTRODUCTION

Wind waves are an important component of climate system and study of their interannual variability helps to understand current climate changes and to assess wave impact in the future. The study of the storminess in the Baltic, Barents and White

Seas have great importance for shipping, constructing on coasts and shelf, oil and gas field development. In this paper, a new approach estimating climate changes has been implemented. We counted a number of storms using significant wave height threshold in three neighbor seas and estimated the connection of storminess

with indices of large-scale atmospheric circulation.

The wave conditions in the Baltic Sea were investigated in several studies (Kriezi and Broman, 2008; Lopatukhin et al. 2006; Medvedeva et al. 2015; Sommere, 2008; Zaitseva-Pärnaste, 2009). Different wave models and wind forcing have been used in these papers. The results of wave simulations have been estimated by comparing with buoy measurements and wave sensors (Kriezi and Broman, 2008; Medvedeva et al. 2016). There are many interesting papers about wave hindcast and climate in the Barents and White Seas (Arkipkin et al. 2015; Korablina et al. 2016; Lopatukhin et al. 2003; Myslenkov et al. 2016; Reistad et al. 2011). Stopa et al. (2016) presented wave climate and hindcast based on altimeter data set and investigation of wave trend in the Arctic region from 1992 to 2014. The decrease of the sea ice extent in the Arctic Ocean over the last years is described in Mokhov (2013). The altimeter data and model results show that the reduction of the sea ice coverage causes a growth of wave heights instead of the increasing wind speeds. However, regional trends are influenced by large-scale interannual climate oscillations like the North Atlantic Oscillation (NAO) and Pacific Decadal Oscillation (Stopa et al. 2016).

The wind and wave climate in the Arctic region based on altimeter measurements were presented by Liu et al. (2016). Trend analysis shows a clear spatial (regional) and temporal (interannual) variability in wave height and wind speed. Wave heights in the Chukchi, Beaufort (near northern Alaska) and Laptev Seas increase at 0.1–0.3 m per decade. These trends have been found statistically significant at the 90% level. The trends of wave heights in the Greenland and Barents Seas, on the contrary, are weak and not statistically significant. In the Barents and Kara Seas, winds and waves increased between 1996 and 2006. Large-scale atmospheric circulation variations such as the Arctic Oscillation (AO) and the Arctic dipole anomaly have a clear impact on the variation of winds and waves in the

Atlantic sector (Liu et al. 2016). Wang (2001) investigated wave heights in the Northern hemisphere and related atmospheric circulation regimes.

In order to take adequate precautions and to reduce risks and damages from the storm the information about the time of occurrence and magnitude of such events is required. This sort of research has been done for other basins of the World Ocean e.g. North Atlantic (De León and Soares, 2015; Rusu et al. 2015). There are a limited number of studies devoted to storm number, their interannual variability and their connection with global atmospheric circulation in the Baltic, Barents and White Seas, so these subject still remains challenging (Korablina et al. 2016; Medvedeva et al. 2015). Our paper focuses mainly on the storm statistics in the Baltic, Barents and White Seas and their connection with large-scale atmosphere circulation indices. The aim of this paper was to compare storm interannual variability in these three neighbor seas and to reveal common and different from each other features and also to assess the connection of storms with indices of large-scale atmospheric circulation.

## MATERIALS AND METHODS

In order to estimate decadal and interannual changes of the wind wave fields the SWAN, short from Simulating WAVes Nearshore, (Booij et al. 1999) and WaveWatch III (Tolman 2009) numerical wave models were used. These models are state-of-the-art and are widely applied for reconstruction of wave fields and such parameters as significant wave heights (in this paper it was considered as mean of 1/3 of the highest waves), periods, lengths, swell heights and energy transport with different spatial and temporal resolutions by solving the energy balance equation (1) in spectral dimensions (Myslenkov et al. 2016; Reistad et al. 2011; Stopa et al. 2016).

For the Baltic and the White Seas the third-generation spectral wind wave model SWAN (version 41.01) has been

implemented in order to obtain wind wave parameters. As a wind forcing we used 10-m wind from Climate Forecast System Reanalysis from the National Centers for Environmental Prediction (NCEP/CFSR) with a spatial resolution  $0.3^\circ \times 0.3^\circ$  and a time step 1 hour (Saha et al. 2010) for the period from 1979 to 2010. Starting from 2011, we used NCEP/CFSv2 (Saha et al. 2014), which is the extension of NCEP/CFSR; it has a spatial resolution  $\sim 0.205^\circ \times 0.204^\circ$  and a time step of 1 hour. The accuracy of the obtained wave parameters is high and it has been estimated by using measurements of the wave parameters (Medvedeva et al. 2016). Accuracy of the model was estimated for the same period, basin and data as in present paper, see details in (Medvedeva et al. 2016): in average  $R$  was 0.96,  $Bias$  0.05,  $RMSE$  0.29 and scatter index 0.18.

For the Barents Sea, the spectral model WaveWatch III version 4.18 has been implemented with an unstructured grid covering the North Atlantic basin and Arctic seas (Fig. 1). "ST1" parametrization has been used for energy input and dissipation. This scheme is based on the same equations that the SWAN configuration used in this study. "DIA" scheme has been implemented for non-linear wave interactions (Hasselmann and Hasselmann, 1985). In addition, WaveWatch allows involving ice coverage. "IC0" scheme has been used for wave energy attenuation in the ice where wave energy reduces exponentially in grid points with ice concentrations between 25% and 75%, otherwise grid points are considered to be open water (<25%) or land (>75%). In WaveWatch III simulations in the Barents Sea we used wind forcing fields and ice concentration from NCEP/CFSR reanalysis from 1979 to 2010 (Saha et al. 2010). This model showed a good agreement with measurements for these regions (Stopa et al. 2016; Tolman 2009). In the White Sea storm statistics was calculated only for days without ice fields. For the Baltic Sea, we didn't exclude any data because Baltic Proper and South-eastern basin usually are not covered by ice.

Calculations have been performed using unstructured grids for the Barents and the White Seas with a spatial resolution 10–20 km in the central and open parts of the seas and 200–500 m in the coastal zones. The unstructured grid for the Barents Sea included the North Atlantic region from the Equator to the North Pole with a spatial resolution  $\sim 1^\circ$  (Fig. 1). The grid for the Baltic Sea was rectangular and had a resolution  $0.05^\circ \times 0.05^\circ$ . The computational grid was created on the basis of the General Bathymetric Chart of the Oceans (GEBCO) with a spatial resolution of one nautical mile for the deep sea. Data from high-resolution navigation maps were used for the bathymetry in coastal zones.

### The model description

The SWAN model is a third-generation spectral wind wave model developed by Delft University of Technology in the Netherlands (Booij et al. 1999) which is traditionally applied for shallow water areas. WaveWatch III has been developed in many research groups, predominantly by the United States' National Oceanic and Atmospheric Administration (NOAA). Based on the same energy balance equation, WaveWatch III is more developed and has more different formulations for the wind input and the whitecapping. It incorporates state-of-the-art formulations for the deep water processes of wave generation, dissipation and the quadruplet wave-wave interactions used by the WAM model (Komen et al. 1994).

The processes included are wind input, whitecapping, bottom friction, depth-induced wave breaking, dissipation due to vegetation, mud or turbulence, obstacle transmission, nonlinear wave-wave interactions (quadruplets and triads) and wave-induced set-up (2).

All information about the sea surface is contained in the wave variance spectrum or energy density  $E(\sigma, \theta)$ , distributing wave energy over (radian) frequencies  $\sigma$  (as observed in a frame of reference moving with current velocity) and propagation directions  $\theta$  (the direction normal to the

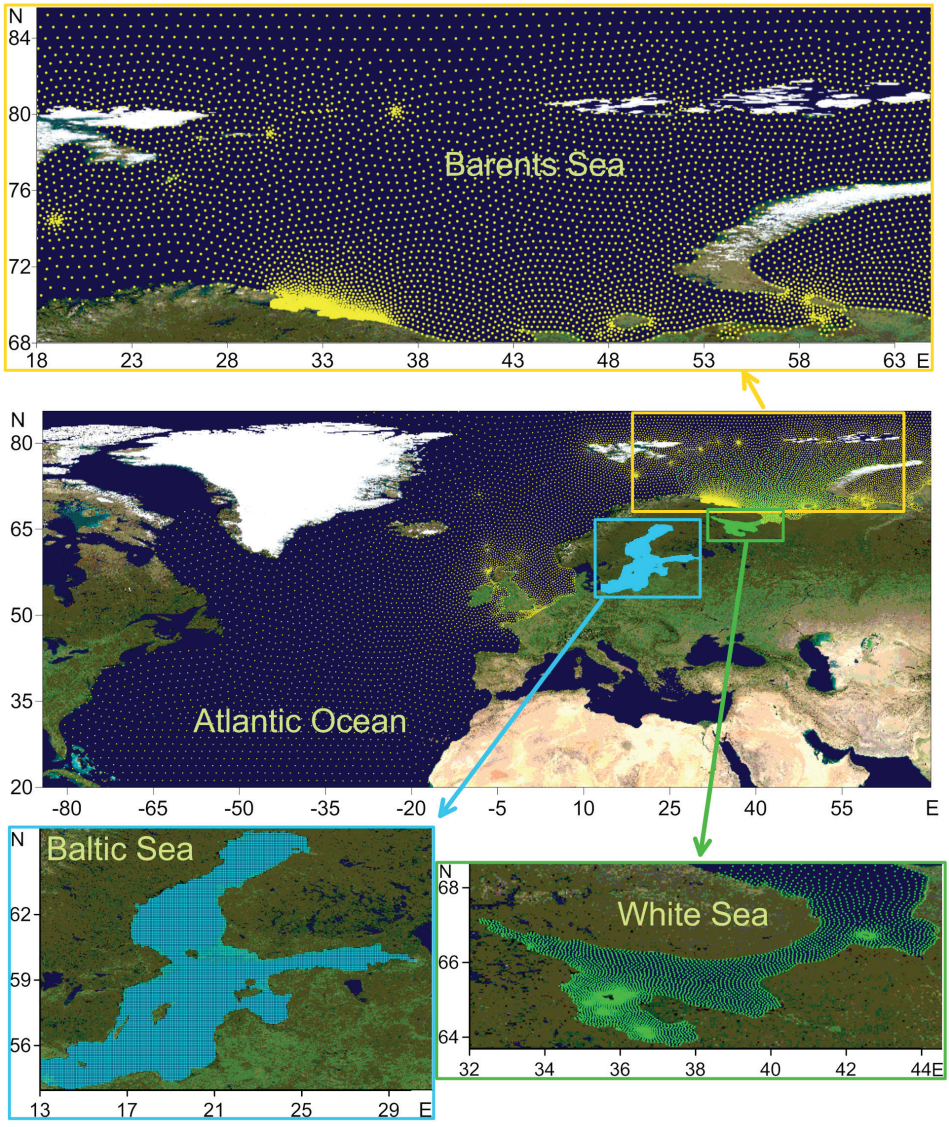


**Fig. 1. The computational grids for the Barents, White and a Baltic Seas**

wave crest of each spectral component). The action density is defined as  $N = E/\sigma$  and is conserved during propagation along its wave characteristic in the presence of ambient current, whereas energy density  $E$  is not.

The evolution of the action density  $N$  is governed by the action balance equation, which reads (Komen et al. 1994):

$$\frac{\partial N}{\partial t} + \nabla_x \cdot [(\vec{c}_g + \vec{U})N] + \frac{\partial c_\sigma N}{\partial \sigma} + \frac{\partial c_\theta N}{\partial \theta} = \frac{Stot}{\sigma} \quad (1)$$

The left-hand side is the kinematic part of this equation. The second term denotes the propagation of wave energy in two-dimensional geographical  $\sim x^2$ -space, with the group velocity  $\sim c_g = \partial \sigma / \partial \vec{k}$  following from the dispersion relation  $\sigma^2 = g|\vec{k}|\tanh(|\vec{k}|d)$  where  $\vec{k}$  is the wave number vector and  $d$  is the water depth. The third term represents the effect of shifting of the radian frequency due to variations in depth and mean currents. The fourth term represents depth-induced and current-induced refraction.

The quantities  $C_\sigma$  and  $C_\theta$  are the propagation velocities in spectral space  $(\sigma, \theta)$ . The right-hand side contains  $S_{tot}$  which is the non-conservative source/sink term that represents all physical processes, which generate, dissipate, or redistribute wave energy. In shallow water, six processes contribute to  $S_{tot}$ :

$$S_{tot} = S_{in} + S_{nl3} + S_{nl4} + S_{ds,w} + S_{ds,b} + S_{ds,br} \quad (2)$$

These terms denote, respectively, wave growth by the wind, nonlinear transfer of wave energy through three-wave and four-wave interactions and wave decay due to whitecapping, bottom friction, and depth-induced wave breaking.

### The model output and storm count

The significant wave heights, periods and wavelengths were reconstructed with wave models for the period from 1979 to 2010 years with a time step of 3 hours for the White and Barents Seas, and for the Baltic Sea – until 2015 with the same time step. Since 2011 year we start to use new version of reanalysis for the Baltic Sea, but the results for the White and Barents Seas in this paper limited by 2010 year, because the calculations with new reanalysis in progress. The main results of wind wave climate investigations (more detailed information about the applied methods, validation and other technical details) for each Sea was presented in recent publications (Arkhipkin et al. 2015; Kislov et al. 2016; Korablina et al. 2016; Medvedeva et al. 2015. 2016; Myslenkov et al. 2015a,b, 2016; Surkova et al. 2013).

All situations when  $H_s$  exceeded the chosen threshold (from 2 to 10 meters) were considered as a storm. The number of storm situations with different significant wave heights was calculated for every year from 1979 to 2010 and respectively 2015. For example, if  $H_s$  in one grid node is higher than 4 meters then it was considered as the start of a storm with criteria  $H_s \geq 4$  m. An event is considered to be finished when the  $H_s$  in all nodes was less than the chosen threshold. When the  $H_s$  reached

the level of 4 meters next time it was considered as another next storm event. A storm with  $H_s \geq 10$  meters is taken into account for each other of the lower criteria from 2 to 10 m and it was included in all these selections. This method of the storm count has some inaccuracy, firstly, when two events happen directly one after

another and, secondly, when in the sea under investigation there are two storms in different parts of the sea. Nevertheless, these cases are not very frequent.

## RESULTS AND DISCUSSION

### Storm number and trends

In the Baltic Sea during 37 years the number of storms with  $H_s \geq 2$  m amounts to 2559, approximately 70 per year, with criteria 3 m – 1285, 4 m – 1107, 5 m – 649. These results indicate that about a half of all storm situations have a significant wave height of more than three meters (Fig. 2).

Typical periods of intensification and relaxation of wind waves are 10–12 years for the Baltic Sea, see Soomere and Räämet (2014). According to the obtained running average of storm number, there is a 10-year period of intensification/weakening of the storm activity. For various parts of the Baltic Sea, there is a discrepancy between the trends of the ten-year increase or decrease. Notably, that the rapid changes of intensification or weakening of wave activity can happen during one decade (Soomere et al. 2008; Broman et al. 2006). In figure 2, the maximum of  $H_s \geq 2$  m was observed in 1983, the local minima are in 1984, 1996 and 2006. For  $H_s \geq 3$  m, the local maxima are in 1983, 1990, 1995 and 2008 years.

There is no significant tendency in storm number in the Baltic Sea with  $H_s \geq 2$  m. However, for criteria  $H_s \geq 4$  m we found a statistically significant negative trend, it amounts -0.17. For storms with  $H_s \geq 3$  m the linear trend of the decrease can be observed in figure 2, but it's not statistically

significant. For 37 years (1979–2015) the maximum computed significant wave height amounts to 8.5 m, wavelength – 130 m, wave period – 10 s.

In the Barents Sea, wind wave conditions are significantly more severe. Four meters were taken as the lowest  $H_s$  threshold for the Barents Sea to calculate storm number, the standard deviation of wave height is about 3 meters for this sea, and thus 4 meters is the lowest level when we can distinguish storm events from noise. Storm number with  $H_s \geq 4$  meters in the Barents Sea is of the same order as storm number with  $H_s \geq 2$  meters in the Baltic having about 80 storms per a year. The maximum of storms with  $H_s \geq 4$  m was observed in 2005 (Fig. 2). For  $H_s \geq 4$  m, local maximum was identified in 2005. The storms with  $H_s \geq 5$  m were registered 40–60 times per a year with local increases in 1989, 1992, 1995 and 2003. For  $H_s \geq 6$  m, there is a local maximum of storms in 1991. For  $H_s \geq 7$  m, the maximum was identified in 1990. There is no significant trend in the Barents Sea detected for the entire period. However, if we divide the period from 1979 to 2010 into 3 segments, we can clearly identify 3 different linear trends for  $H_s \geq 6$  m (Fig. 2a). From 1979 to 1991 the quantity of storms increases, from 1992 to 2002 it decreases and then not great augmentation again occurs. Thus for the Barents Sea, the same period as in the Baltic Sea about 10–12 years was identified. For 32 years (1979–2010) the maximum computed significant wave height is 16 m (at the west boundary, 25°E). The same analysis was carried out for the White Sea. In the central open part of the White Sea, the number of storms with  $H_s \geq 2$  m is about 20 times per a year for the ice-free period (Fig. 2). As for storms with  $H_s \geq 3$  m, they occurred only 5–6 times per year. Interannual variability of the number of storms in the White Sea is less determined than in the Barents, but for  $H_s \geq 2$  m there is a maximum in 1995 and a minimum in 1999. Since 1999, the storm number increases, but positive trend in storminess isn't significant. For  $H_s \geq 3$  m, there are two maxima in 1986 and 1994, two minima in 1985 and 1999.

In the White Sea, the following features of the wave climate are observed: the maximum of number of storms in the autumn and winter months, a significant spatial and temporal heterogeneity of the properties of wind wave fields, where each part of the sea such as Onega Bay, Basin, Gorlo, and Voronka has their own determined wave mode.

In addition, the relations of storm number between different Seas was studied. It is interesting that the highest significant correlation (0.56) was discovered between the storm number, discussed above, of the Barents storms with  $H_s \geq 7$  m and Baltic storms with  $H_s \geq 4$  m, which have statistically significant negative trend. These events occur about 20 times per a year. For others Baltic storms with  $H_s \geq 3$ , 5 m and Barents events with  $H_s \geq 5$ , 6, 8 m  $R$  was also approximately 0.5. We can make a supposition that it reflects the connection of these processes and its common origin. For more severe Barents storms with upper thresholds 9 and 10 m the link  $R = 0.52$  m is observed with the White Sea storms with  $H_s \geq 3$  m level (about 5 times per a year), however this connection is reflected only on scales of greater wave heights and isn't observed with the Baltic Sea. All other correlation coefficients are small. So high correlation is not observed between White and Baltic Seas at all. And for events with  $H_s \geq 2$  m it was not revealed too.

The relations of storm number with atmospheric indices. In order to study the connection with the global atmospheric circulation, 3 indices North-Atlantic Oscillation (NAO), Arctic Oscillation (AO), Scandinavian Index (SCAND) have been considered. The correlation coefficient ( $R$ ) was calculated between these indices and the max  $H_s$ , the results are presented in table 1.

We will regard as the state of the atmosphere with a positive value of the NAO index as the positive phase of the oscillation and when the value is below zero – as negative (<http://www.cpc.ncep.noaa.gov/> 2017). In the positive phase of the oscillation, the Icelandic minimum and

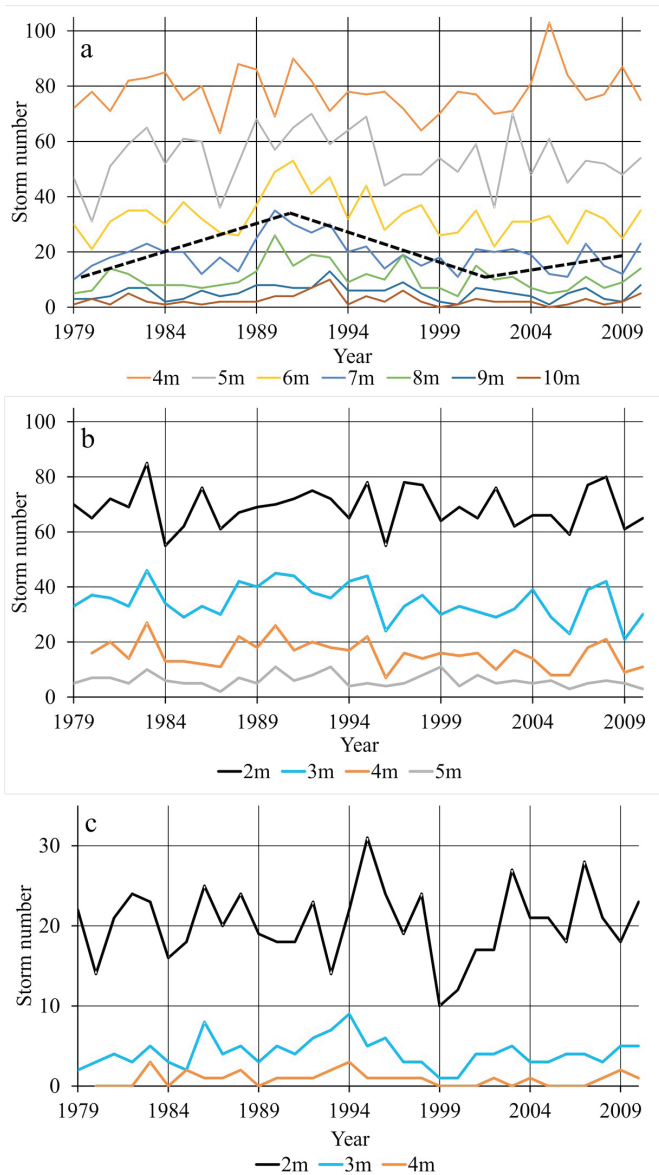


**Fig. 2. The number of storms with the different  $H_s$  for the Barents (a), Baltic (b) and White Seas (c)**

the Azores maximum are well developed, the pressure gradients between them are increased, the zonal circulation is strengthened. In the negative phase, there is a weakening of the zonal transport and an intensification of the meridional processes.

The AO is a large-scale mode of climate variability also referred to as the Northern Hemisphere annular mode (<http://www.cpc.ncep.noaa.gov/> 2017).

The AO is a climate pattern characterized by winds circulating counterclockwise around the Arctic at around 55°N latitude. When the AO is in its positive phase, a belt of strong winds circulating around the North Pole acts to confine colder air across Polar Regions. This belt of winds becomes weaker and more distorted in the negative phase of the AO, which allows an easier southward penetration of colder, arctic air

**Table 1. The coefficient of correlation  $R$  between mean annual storm number with different  $H_s$  threshold for the Baltic, White and Barents Seas and mean annual indices of large-scale atmospheric circulation. Bold font indicates significant  $R$**

Baltic Sea				White Sea				Barents Sea			
$H_s \geq$	NAO	AO	SCAND	$H_s \geq$	NAO	AO	SCAND	$H_s \geq$	NAO	AO	SCAND
2 m	0.12	0.32	<b>-0.59</b>	2 m	-0.07	-0.02	-0.29	4 m	0.12	0.09	0.16
3 m	0.42	0.49	<b>-0.47</b>	3 m	0.18	0.2	0.06	5 m	0.44	<b>0.45</b>	-0.24
4 m	0.35	<b>0.45</b>	<b>-0.52</b>					6 m	0.27	0.35	-0.33
5 m	0.28	<b>0.36</b>	-0.32					7 m	0.35	<b>0.47</b>	-0.23
2 m (by NCAR)	0.31	<b>0.46</b>	<b>-0.48</b>					8 m	0.21	0.42	-0.19
								9 m	0.18	0.36	0.11
								10 m	0.03	0.11	-0.02

masses and increased storminess into the mid-latitudes.

The Scandinavia pattern SCAND consists of a primary circulation center over Scandinavia, with weaker centers of opposite sign over Western Europe and eastern Russia/ western Mongolia. The Scandinavia pattern has been previously referred to as the Eurasia-1 pattern by (Barnston and Livezey 1987). The positive phase of this pattern is associated with positive height anomalies, sometimes reflecting major blocking anticyclones, over Scandinavia and western Russia, while the negative phase of the pattern is associated with negative height anomalies in these regions. The positive phase of the Scandinavia pattern is associated with below-average temperatures across central Russia and also over western Europe. It is also associated with above-average precipitation across central and southern Europe and below-average precipitation across Scandinavia.

Correlation analysis of the mean annual number of the storm and mean annual indices of atmospheric circulation is presented in table 1. It showed that connection of storm number in the Barents Sea  $R$  about 0.5 is only with AO, for  $H_s \geq 5$  m (0.45) and  $H_s \geq 7$  m (0.49). However, if we consider not annual but

winter averaged monthly index AO (DJFM) and monthly values of storm number, then, in the Barents Sea, the connections between a number of storms and AO on decadal scales is reflected better. The highest correlation coefficient between AO index (averaged from December to March)  $R$  (0.6) was obtained for storms with  $H_s \geq 7$  m (Fig. 3a), and for  $H_s \geq 8$  m with AO it amounts to 0.57. With SCAND pattern the link isn't observed.

For the White Sea, the relations between a number of storms and AO, NAO indices are weak (Fig. 3c, d). Maximum  $R = 0.26$  and other coefficients are less. The liaison between storm number in the Barents and White Seas and SCAND pattern is weak and it was not revealed.

For the Baltic Sea the connection of storm number is mostly pronounced with SCAND. The highest correlation is -0.59 for  $H_s \geq 2$  m (Table 1). Also  $R$  with AO reaches 0.45-0.49 for different thresholds. Summarizing this section, we can say that the connection with indices of global atmospheric circulation is mostly developed for the Baltic Sea with SCAND pattern, less with AO. Secondly, it is reflected in the Barents Sea with AO. For the White Sea such link was not revealed.

Fig. 3 (e, f) shows good correspondence for the Baltic Sea annual storm number and NAO, AO indices. However, maximum  $R$  amounts 0.49 for the storm number with  $H_s \geq 3$  m and it was revealed with AO. For events with  $H_s \geq 4$  m, it amounts 0.45. With NAO the connection is not obvious. As for SCAND pattern, it is worth noting that  $R$  is the highest but it is negative about -0.59 for  $H_s \geq 2$  m, -0.52 for  $H_s \geq 4$  m, and -0.47 for  $H_s \geq 3$  m (Table 1). It means that the increase in storm number over the Baltic Sea corresponds to the negative phase of the Scandinavian pattern associated with negative height anomalies in this region.

The connections between a number of storms with positive and negative NAO, AO and SCAND phases are shown in fig. 4. It shows that there is no positive or negative significant trend in a number of storms with  $H_s \geq 2$  m. For comparison, (Medvedeva et al. 2015) showed a similar trend, but the simulations were based

on other reanalysis data NCEP/NCAR (Kalnay et al. 1996). They had a longer time coverage from 1948 to 2010 but less accuracy of the modeled results and errors are twice as high. Previous versions of the reanalysis data have shown an increase in storm activity and an obvious 20-year periodicity. In figure 3, we noted the decrease of stronger storms shown by linear trends. There is only one trend corresponding to  $H_s \geq 4$  m, which is statistically significant by Fisher criteria. To compare with the previous version of the reanalysis (NCAR) the coefficient  $R$  with AO is lower and amounts to 0.46 (with CFSR 0.49). With NAO and SCAND NCAR reanalysis shows worse correlation.

### The relations of maximum $H_s$ and storm number with atmospheric indices for regions of the Baltic Sea

The commonly accepted reasons behind the possible increase in the Baltic Sea

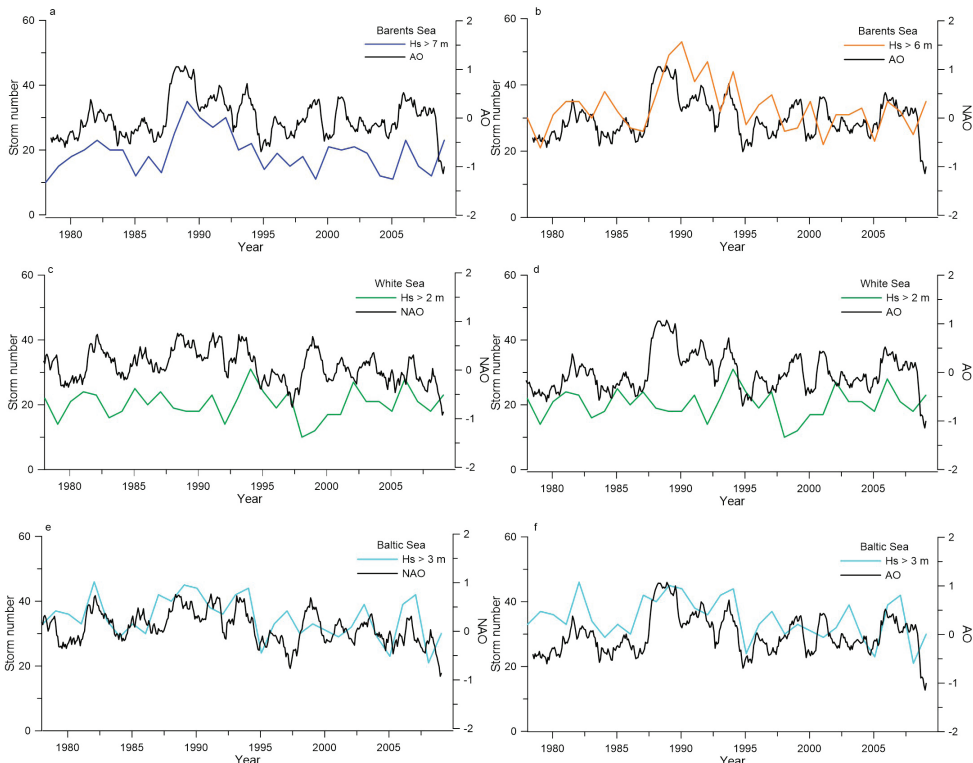


**Fig. 3. Connections between indices AO, NAO and the number of storms in the Barents (a, b), White (c, d) and Baltic Seas (e, f). Indices are presented by running average with 13 months values**

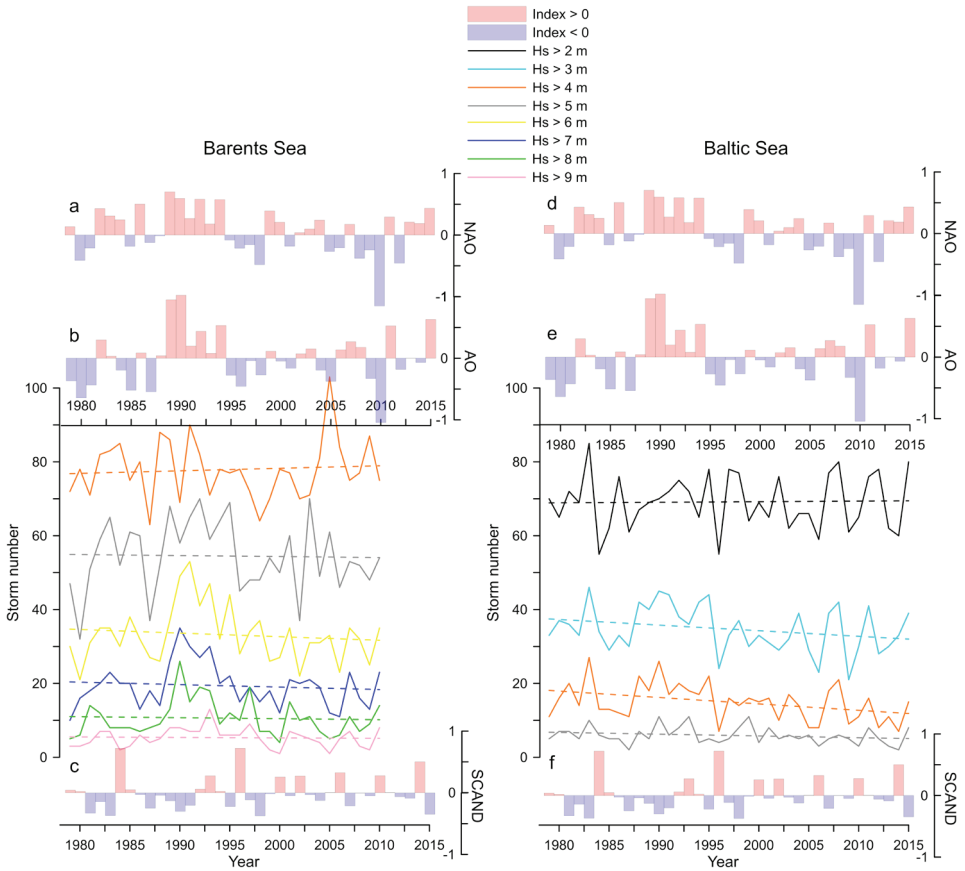


**Fig. 4. Storm number with different  $H_s$  threshold for the Barents (a-c) and Baltic (d-f) Seas with the NAO, AO, SCAND indices. The dashed line represents linear trends**

wave heights are 1) a reduction of sea ice in northern parts of the sea and 2) an increase in the wind speed (Hünicke et al. 2015). Both these reasons should lead to a spatially inhomogeneous increase in the wave heights, first of all in seasonally ice-covered northern part of the Sea and along the eastern segments of the basin where the predominant south-westerly and north-north-westerly winds usually create the severest wave conditions. Analysis of Kudryavtseva and Soomere (2017) reveals an unexpected strong meridional pattern of changes: the wave heights have increased in the western offshore of the sea and have decreased (or exhibit no changes) along the eastern nearshore. It is, therefore, unlikely that a discernable increase in the wind speed has occurred in this region. This among other things means that a greater level

of storms and swells (Bertin et al. 2013) may only characterize some parts of the North Atlantic. This is consistent with the conclusion that the basin-wide average geostrophic wind speed has not increased over the entire Baltic Sea (Soomere and Räämet, 2014).

In this paper the entire Baltic Sea was divided into 5 areas (Fig. 5): the South-Eastern Baltic (I), the Gulf of Bothnia (II), the Gulf of Finland (III), the Gulf of Riga (IV) and the Baltic Proper (V) (Fig. 5) and the maximum  $H_s$  was identified for each part for every month (2200 values in all). As maximum  $H_s$ , we considered maximum value registered in this area for a selected period (for example the maximum value of  $H_s$  in one node in the Gulf of Finland in January 1990). Then for every month of this period from January to December, the

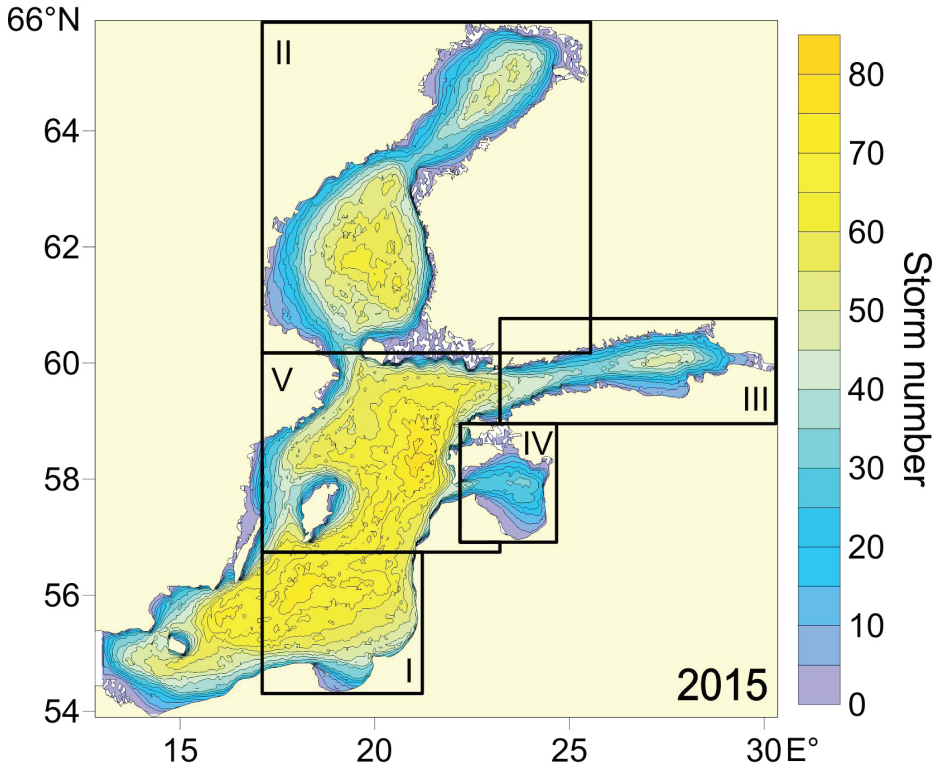


**Fig. 5. Map of the yearly distribution of the storm numbers in every node in 2015 with 5 areas in which trends of max  $H_s$  and storm number were estimated: I – the Southeastern Baltic (in rectangular from Slupsk to Liepaja), II – the Gulf of Bothnia (including the Bothnian Bay and the Bothnian Sea), III – the Gulf of Finland, IV – the Gulf of Riga, V – the Baltic Proper**

maximum  $H_s$  was selected (444 values in all).

For the Baltic Sea in the cold season, the field variability connected to the NAO is most pronounced. If we take into account only the period from December to March (with  $R \geq 0.5$ ), the connection of max  $H_s$  is more significant with AO, slightly less significant with NAO and negative (-0.4; -0.5) with SCAND (Table 2).

We observe a positive high correlation coefficient of  $\geq 0.5$  with the NAO index for five months: January, February, March and April, and for the Baltic Proper for November. For all other months, it has a low value close to the zero or negative. The highest value of  $R = 0.7$  was observed for December in the Gulf of Finland (Fig. 6, Table 2). It is evident from the figures 3, 4, that every increase of

the  $H_s$  in the Gulf of Finland corresponds to the positive phase of the NAO and AO indices. It is obvious that with positive NAO the number of deep cyclones over the North Atlantic region increases and maximum  $H_s$  increase too. Negative NAO phase in most cases coincides with the  $H_s$  decrease.

The AO index  $R \geq 0.5$  was identified for the winter period (plus April), the maximum value equals 0.64 for the Southeastern part of the Baltic Sea for January. In the spring-autumn period, the link is not obvious.

All coefficients  $R$  with the SCAND are negative. Notably, for January, February, April, and September with  $R \leq -0.5$ , i.e. the  $H_s$  increases with the negative phase of the index. The highest values of  $R$ -0.67, -0.65 are found in the Southeastern part of the Baltic Sea.

**Table 2. Correlation coefficient *R* calculated between the value of max *H<sub>s</sub>* (for a month) and monthly indices of large-scale atmosphere circulation (NAO, AO, SCAND). The bold font indicates significant *R***

Month	1	2	3	11	12	
NAO	<b>0.47</b>	0.29	<b>0.57</b>	-0.05	<b>0.59</b>	Southeastern Baltic
	0.18	<b>0.53</b>	<b>0.55</b>	-0.01	0.43	Gulf of Bothnia
	0.36	<b>0.54</b>	<b>0.55</b>	-0.04	<b>0.70</b>	Gulf of Finland
	0.44	<b>0.49</b>	<b>0.49</b>	0.11	<b>0.65</b>	Gulf of Riga
	<b>0.52</b>	0.38	<b>0.57</b>	<b>0.55</b>	<b>0.60</b>	Baltic Proper
AO	<b>0.64</b>	<b>0.54</b>	<b>0.51</b>	0.27	0.44	Southeastern Baltic
	0.17	<b>0.49</b>	<b>0.47</b>	0.07	<b>0.49</b>	Gulf of Bothnia
	<b>0.57</b>	<b>0.55</b>	<b>0.58</b>	0.21	<b>0.56</b>	Gulf of Finland
	<b>0.50</b>	<b>0.57</b>	<b>0.55</b>	0.30	<b>0.50</b>	Gulf of Riga
	<b>0.56</b>	<b>0.55</b>	<b>0.50</b>	<b>0.49</b>	<b>0.58</b>	Baltic Proper
SCAND	<b>-0.67</b>	<b>-0.65</b>	-0.40	<b>-0.45</b>	-0.37	Southeastern Baltic
	-0.19	<b>-0.45</b>	-0.21	<b>-0.45</b>	-0.31	Gulf of Bothnia
	-0.41	<b>-0.57</b>	-0.31	-0.43	-0.28	Gulf of Finland
	-0.42	<b>-0.46</b>	-0.39	-0.39	-0.27	Gulf of Riga
	<b>-0.60</b>	<b>-0.58</b>	-0.35	-0.32	-0.35	Baltic Proper

From the geographical perspective the highest *R* was noted in the Gulf of Finland (Fig. 6, Table 2) as with NAO, so with AO. For this area, the maximum value for NAO corresponds to December (*R* = 0.7) and for AO in March (0.68). Thus, with such complex configuration of the Baltic Sea, the NAO and AO indices have the most influence on the Gulf of Finland and secondly on the Baltic Proper. The lowest *R* coefficients were observed for the Gulf of Bothnia. It is worth noting, that in the last decade from 2005 to 2015 the storm number with *H<sub>s</sub>* ≥ 2, 3, 4 m increases in the entrance of the Gulf of Finland. This conclusion is based on obtained results and on analysis of maps of maximum *H<sub>s</sub>* distribution (constructed for every month for every year). In addition, it propagates deeper to the east, so it reflects the displacement of the trajectories of cyclones, which have moved 5° to the north. It changes the length of the wave fetch and promotes wave penetration into the Gulf of Finland.

As for storm number in separate parts of the sea (Table 3), the highest *R* is noted in the Baltic Proper with AO for *H<sub>s</sub>* ≥ 3 m and *R* equals 0.62. For storm events with *H<sub>s</sub>* ≥ 4 m, the situation is the same: the correlation for the Baltic Proper is stronger 0.54.

Summarizing, the connection between significant wave height and indices is stronger in the Baltic Proper and it was observed in more months than in any other part of the sea, th Baltic Proper is on the second place. If we consider the absolute value of correlation, in the Gulf of Finland *R* amounts 0.7 in the December.

As for seasonal variability of correlation – the connection is more determined from November to March with a maximum in the February.

If we take into account, storm number separately calculated for parts of the Baltic then in the Baltic Proper *R* is higher.

**Table 3. The correlation coefficient between the number of storms and indices of atmospheric circulation in different parts of the Baltic Sea. The bold font shows significant  $R \geq 0.5$**

<i>R</i>	NAO	AO	SCAND
<i>H<sub>s</sub> ≥ 2 m</i>			
Southeastern Baltic	0.08	0.23	<b>-0.56</b>
Gulf of Bothnia	0.26	0.41	<b>-0.50</b>
Gulf of Finland	0.32	0.43	-0.19
Gulf of Riga	<b>0.43</b>	<b>0.54</b>	-0.26
Baltic Proper	0.17	0.35	<b>-0.61</b>
<i>H<sub>s</sub> ≥ 3 m</i>			
Southeastern Baltic	0.41	<b>0.46</b>	<b>-0.48</b>
Gulf of Bothnia	0.32	<b>0.48</b>	<b>-0.47</b>
Gulf of Finland	<b>0.51</b>	<b>0.55</b>	-0.39
Gulf of Riga	<b>0.46</b>	<b>0.45</b>	-0.25
Baltic Proper	0.42	<b>0.62</b>	<b>-0.49</b>
<i>H<sub>s</sub> ≥ 4 m</i>			
Southeastern Baltic	0.28	0.33	-0.16
Gulf of Bothnia	0.33	0.35	-0.17
Gulf of Finland	0.40	0.41	-0.27
Baltic Proper	0.43	<b>0.54</b>	<b>-0.37</b>

### Future changes

The climate projection of weather pattern accompanying extreme winds over the Barents and Baltic Seas is carried out with the database of CMIP5 models ensemble runs (RCP8.5 scenario), see Moss et al. 2008; Taylor et al. 2012. According to this scenario, the global surface air temperature will be 3.5-4°C higher than in 1961-1990. The key idea relies upon the “environment – to circulation” method (Huth et al. 2008). It is based on the assumption that extreme weather phenomena (local or mesoscale) are connected through physical mechanisms with large-scale (synoptic) events. Then it is possible to make projections indirectly, studying configuration and intensity of sea level atmospheric pressure (SLP) fields which are supposed to be the determining factor of the wind speed and thus of wind waves. In this way, there is no need to run

a wave model for the future climate, but to look into the climate projection for the fields of SLP, which are associated with storm situations in the modern climate.

Due to cyclonic activity in high latitudes, strong winds and stormwind waves are frequently observed there all year round, especially, in the cold season. For the severe and specific climate of the Barents and Baltic Seas, it is complicated to adequately observe directly the atmosphere and ocean and even to use information from satellites. In this case, weather and climate models are of great value to understanding the present atmosphere-ocean interaction processes and their physical mechanisms. Earth system modeling is an important instrument for future climate projection of extreme weather events, which should help to identify and manage the risks of extreme events (Field et al. 2012).

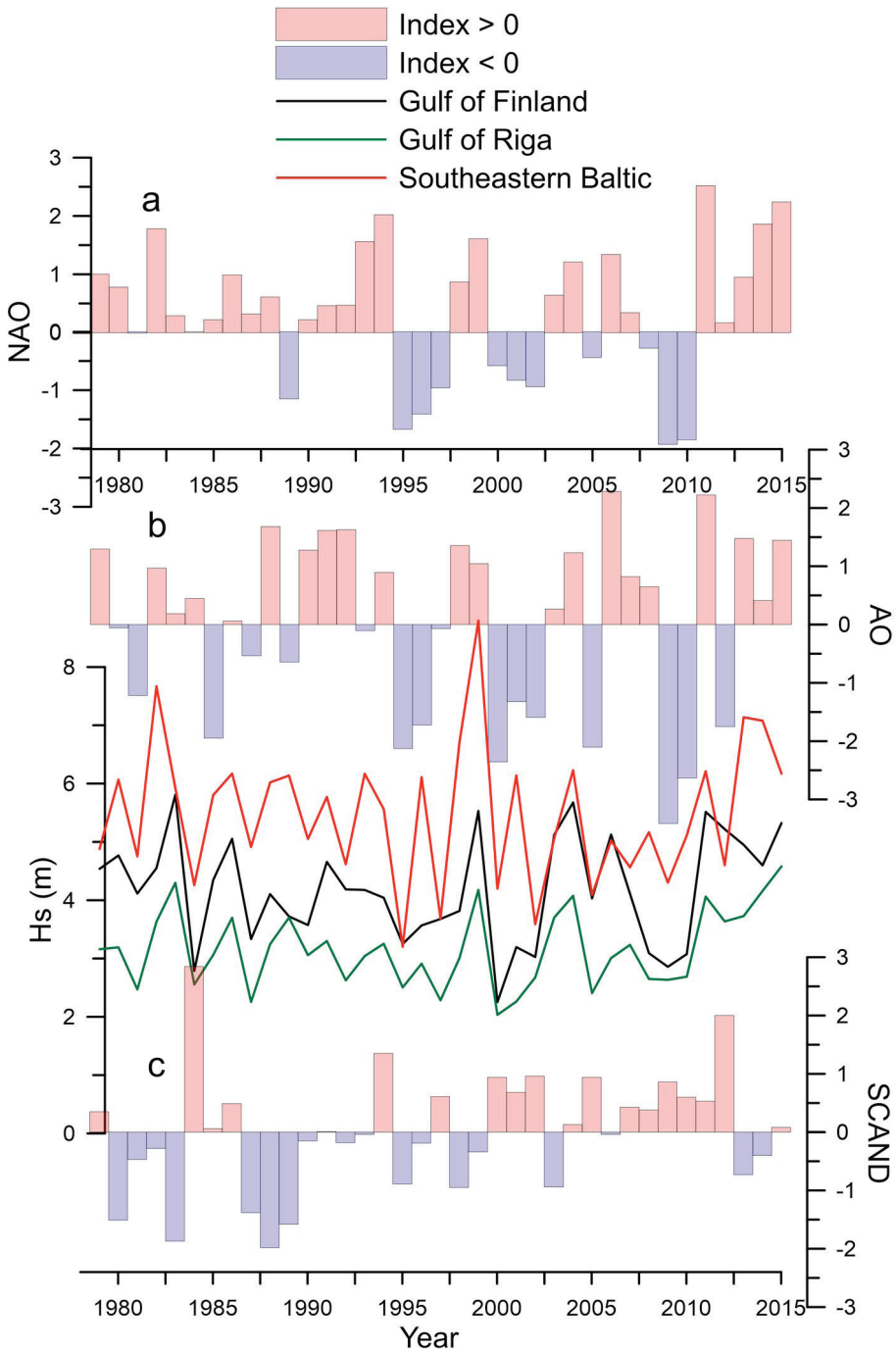


**Fig. 6.** Storm number with different  $H_s$  threshold for the Barents (a-c) and Baltic (d-f) Seas with the NAO, AO, SCAND indices. The dashed line represents linear trends Interannual variability of maximum significant wave heights in the Gulf of Finland (black line), Baltic Proper (red line) and Gulf of Riga (green line) for December from 1979 to 2015 with 3 indices of large-scale atmospheric circulation; NAO (a), AO (b), SCAND (c).

To make a projection of extreme events in the future we applied the original method described in Surkova et al. (2013), Surkova and Krylov (2017). We used two approaches to get the calendar of these events for the last decades. For the Baltic Sea, a calendar of storms was derived from results of experiments of the wave model SWAN for 1948–2011. We choose such days when the modeled  $H_s$  was 4 m or higher (the government standard of general requirements for safety in emergencies specifies waves with a height of 4 m or more in the coastal zone and 6 m or more in the open sea as hazardous ones). For the Barents Sea, we considered a day as an extreme event when the wind speed was higher than the value of its 99th percentile. We found 364 events for the Baltic Sea (1950–2010) and 240 events for the Barents Sea (1981–2010).

Based on these calendars, a catalog of atmospheric SLP fields was prepared for each sea. The data used was the one of NCEP/NCAR reanalysis (Kalnay et al. 1996) for the Baltic Sea, and ERA-Interim for the Barents Sea (Dee et al. 2011). Every storm SLP field from reanalysis then was compared with everyday models SLPs of 1950–2005 period for every climate model (24 CMIP5 models for the Baltic Sea and

27 models for the Barents Sea). When for the present climate the SLP from the climate model had a coefficient of spatial correlation  $R$  more than the critical one  $R_c$  and the same spatial variance as the storm field it was taken into account. It was found that when  $R_c \geq 0.97$ –0.98 (individually calculated for each model) the number of storm events simulated by the model is as many as in the storm calendar.

Then analogs of “storm SLP fields” and their frequency were investigated for the climate models results for an RCP8.5 CMIP5 experiment for 2006–2100. For this period the days were chosen when the correlation of modeled SLP and storm SLP from reanalysis was higher than  $R_c$ .

The results show (Fig. 7) that the frequency of extreme weather events connected with high wind speed and wind waves can shift towards higher values over the Baltic and Barents Seas according to most climate models in the case of the increasing global warming under scenario RCP8.5.

## CONCLUSIONS

The numerical model simulations of storm activity in the White, Baltic and Barents Seas were analyzed. From 1979 to 2015

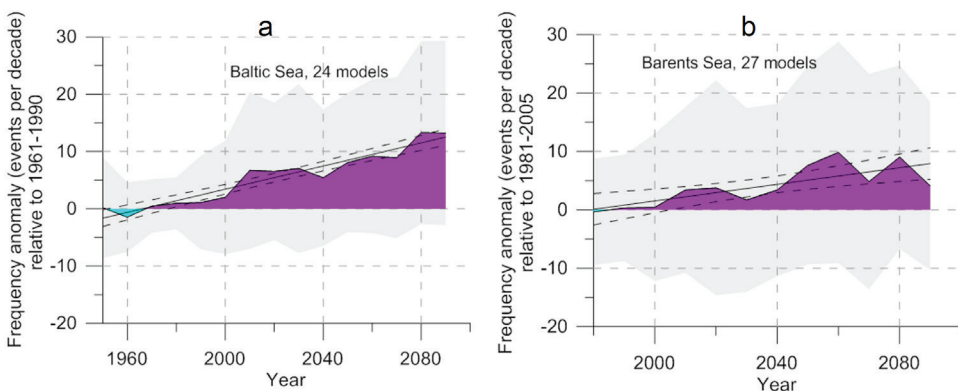


**Fig. 7. Frequency anomaly (events per decade) of SLP patterns forcing high wind waves over the Baltic Sea (a) and high wind speed over the Barents Sea (b). The number of CMIP5 models used to calculate the multi-model mean is indicated on graphs. The CMIP5 multi-model mean is given by the light and dark blue filling. The trend is a straight solid line, its significance at the 5% level is shown by the dashed lines. Multi-model ensemble range is indicated by grey shaded bands (within 3-sigma limits)**

the number of storms with different  $H_s$  threshold was calculated. High interannual variability is observed for all studied seas. The storm conditions in the Barents Sea is significantly more severe in comparison with the other considered seas. The storm number with  $H_s \geq 2$  m in the Baltic is comparable with storm number with  $H_s \geq 4$  m in the Barents Sea: an average 80 per year. The number of storms in the White Sea is four times lower: ~20 per a year with  $H_s \geq 2$  m. In the Barents Sea, the most severe storms have threshold  $H_s \geq 10$  m, which even doesn't occur in the Baltic and White Seas. For the Baltic, the considered limit was 5 m (5-7 per a year) and for the White Sea – only 4 m (2-3 per a year).

There is no significant trend of storm number in the Baltic, Barents and White Seas detected for the entire period. For the Barents and Baltic Seas the variability period about 10–12 years was identified. In the Baltic and Barents Seas, the small-scale increase of the number of storms was found in 1992–1994 years. It corresponds to the high positive NAO and AO and significant negative SCAND values. For the White Sea, the positive NAO phase in contrary corresponds to the decrease of the storm number. On average, the connection with global atmospheric circulation is stronger ( $R \geq 0.5$ ) for the Baltic Sea, then for the other two seas. The most pronounced liaison for the Baltic is with SCAND pattern, for the Barents – with AO. The connection with AO index is clearer than with NAO for all three seas. Notably, that for stronger storms with  $H_s \geq 4$  m in the Baltic the significant negative linear trend was identified. It is interesting that the number of these events is connected

with Barents storms with  $H_s$  threshold 7 m and correlation between them is 0.56. Also correlation of number of stronger storms in the Barents Sea ( $H_s \geq 8, 9$  m) and storm number of the White Sea ( $H_s \geq 3$  m) is significant (0.52). It reflects the common origin of these events.

According to the RCP8.5 scenario, in the second part of the XXI century the number of storm events will rise in the Baltic and Barents Seas.

## ACKNOWLEDGMENTS

The results of part 1 (Storm number and trends) were obtained in the framework of the state assignment of FASO Russia (theme No. 0149-2018-0015). The results of part 2 (The relations of storm number with atmospheric indices) were obtained within the Russian Science Foundation grant (project No.14-50-00095). The results of part 3 (The relations of maximum  $H_s$  and storm number with atmospheric indices for regions of the Baltic Sea) were obtained within the Russian Foundation for Basic Research grant (project No. 16-35-00338). The results of part 4 (Future changes) were obtained within the Russian Science Foundation grant (project No. 14-37-00038).

«S. Myslenkov and S. Zilitinkevich acknowledge support from the Academy of Finland projects ABBA No. 280700 (2014-2017); S. Zilitinkevich acknowledges support from the Academy of Finland project ClimEco No. 314 798/799 (2018-2020) and RSF project No. 15-17-20009 (2015-2018)». ■

## REFERENCES

- Arkhipkin V., Dobrolyubov S., Myslenkov S., and Korablina A. (2015). The Wave Climate of the White Sea, Changing Climate and Socio-Economic Potential of the Russian Arctic. In: S. Sokratov, ed., 1st ed. Moscow: Liga-Vent, pp.48-58 (in Russian with English summary).
- Barnston A. and Livezey R. (1987). Classification, seasonality, and persistence of low-frequency atmospheric circulation patterns. *Monthly weather review*, 115(6), pp. 1083-1126.
- Bertin X., Prouteau E., and Letetrel C. (2013). A significant increase in wave height in the North Atlantic Ocean over the 20th century. *Global and Planetary Change*, 106, pp. 77-83.
- Booij N., Ris R., and Holthuijsen L. (1999). A Third-Generation Wave Model for Coastal Regions. 1. Model Description and Validation. *Journal of geophysical research: Oceans*, 104(C4), pp.7649-7666.
- Broman B., Hammarklint T., Rannat K., Soomere T., and Valdmann, A. (2006). Trends and extremes of wave fields in the north-eastern part of the Baltic Proper. *Oceanologia*, 48(S), pp.165-184.
- Dee D., Uppala S., Simmons A., Berrisford P., Poli P., Kobayashi S., ..., and Bechtold P. (2011). The ERA-Interim reanalysis: configuration and performance of the data assimilation system, *QJ Roy. Meteor. Soc.*, 137, pp. 553–597.
- De León, S., and Soares, C. (2015). Hindcast of the Hércules winter storm in the North Atlantic. *Natural Hazards*, 78(3), pp.1883-1897.
- Field C., Barros V., Stocker T., Qin D., Dokken D., and Ebi K. (2012). IPCC 2012. Managing the risks of extreme events and disasters to advance climate change adaptation. A special report of the intergovernmental panel on climate change. Cambridge University Press. Cambridge: Cambridge University Press.
- Hasselmann S. and Hasselmann K. (1985). Computations and parameterizations of the nonlinear energy transfer in a gravity-wave spectrum. Part I: A new method for efficient computations of the exact nonlinear transfer integral. *Journal of Physical Oceanography*, 15(11), pp.1369-1377.
- National Weather Service Climate Prediction Center (2017). [online] Available at: <http://www.cpc.ncep.noaa.gov/> [Accessed 01 Nov. 2017].
- Hünicke B., Zorita E., Soomere T., Madsen K. S., Johansson M., and Suursaar Ü. (2015). Recent change—Sea level and wind waves. In *Second Assessment of Climate Change for the Baltic Sea Basin* (pp. 155-185). Springer, Cham.
- Huth R., Beck C., Philipp A., Demuzere M., Ustrnul Z., Cahynová M., Kyselý J., and Tveito O. (2008). Classifications of Atmospheric Circulation Patterns Recent Advances and Applications. *Trends and Directions in Climate Research*, Ann. N.Y. Acad. Sci., 1146(1), pp.105-152. DOI: 10.1196/annals.1446.019.
- Kalnay E., Kanamitsu M., Kistler R., Collins W., Deaven D., Gandin L., ..., and Zhu Y. (1996). The NCEP/NCAR 40-year reanalysis project. *Bulletin of the American meteorological Society*, 77(3), pp. 437-471.
- Kislov A., Surkova G., and Arkhipkin V. (2016). Occurrence Frequency of Storm Wind Waves in the Baltic, Black, and Caspian Seas under Changing Climate Conditions. *Russian Meteorology and Hydrology*, 41(2), pp.121-129 (in Russian).
- Komen G., Cavaleri L., Donelan M., Hasselmann K., Hasselmann S., and Janssen P. (1994). *Dynamics and modeling of ocean waves*. Cambridge: Cambridge University Press.

Korablina A., Arkhipkin V., Dobrolyubov S., and Myslenkov S. (2016). Modeling storm surges and wave climate in the White and Barents Seas. In Saint-Petersburg, Russia: EMECS 11 – Sea Coasts XXVI Joint Conference «Managing Risks to Coastal Regions and Communities in a Changing World», 2016, pp.184-194. DOI: 10.21610/conferencearticle\_58b4317442aca

Kriezi E. and Broman B. (2008). Past and future wave climate in the Baltic Sea produced by the SWAN model with forcing from the regional climate model RCA of the Rossby Centre. In US/EU-Baltic International Symposium, 2008 IEEE/ OES, pp. 1-7.

Kudryavtseva N. and Soomere T. (2017). Satellite altimetry reveals spatial patterns of variations in the Baltic Sea wave climate. arXiv preprint arXiv:1705.01307.

Liu Q., Babanin A., Zieger S., Young I., and Guan C. (2016). Wind and Wave Climate in the Arctic Ocean as Observed by Altimeters. *Journal of Climate*, 29(22), pp.7957-7975.

Lopatukhin L., Buhanovskij A., Degtyarev A., and Rozhkov V. (2003). Reference data of wind and waves climate of the Barents, Okhotsk, and Caspian Seas. Russian Maritime Register of Shipping, Saint-Petersburg: SPB (in Russian).

Lopatukhin L., Buhanovskij A., Ivanov S., and Chernysheva E. (2006). Reference data on the regime of wind and waves of the Baltic, Northern, Black, Azov and Mediterranean Seas. Russian Maritime Register of Shipping. Saint-Petersburg: SPB (in Russian).

Medvedeva A., Arkhipkin V., Myslenkov S., and Zilitinkevich S. (2015). Wave climate of the Baltic Sea following the results of the SWAN spectral model application. *Moscow University Bulletin. Series 5. Geography* (1), pp.12-22 (in Russian with English summary).

Medvedeva A., Myslenkov S., Medvedev I., Arkhipkin V., Krechik V., and Dobrolyubov S. (2016). Numerical Modeling of the Wind Waves in the Baltic Sea using the Rectangular and Unstructured Grids and the Reanalysis NCEP/CFR. *Proceedings of the Hydrometeorological Research Center of the Russian Federation* (362), pp. 37-54 (in Russian with English summary).

Mokhov I., Semenov V., Khon V., and Pogarsky F. (2013). Change of sea ice content in the Arctic and the associated climatic effects, detection and simulation. *Led i Sneg*, 53(2), pp. 53-62.

Moss R., Babiker W., Brinkman S., Calvo E., Carter T., Edmonds J., ... and Jones R. N. (2008). *Towards New Scenarios for the Analysis of Emissions: Climate Change, Impacts and Response Strategies*.

Myslenkov S., Arkhipkin V., and Koltermann K.P. (2015a). Evaluation of swell height in the Barents and White Seas. *Moscow University Bulletin. Series 5. Geography* (5), pp. 59-66 (in Russian with English summary).

Myslenkov S., Platonov V., Toropov P., and Shestakova A. (2015b). Simulation of storm waves in the Barents Sea. *Moscow University Bulletin. Series 5. Geography* (6), pp.65-75 (in Russian with English summary).

Myslenkov S.A., Golubkin P.A. and Zabolotskikh E.V. (2016). Evaluation of wave model in the Barents Sea under winter cyclone conditions. *Moscow University Bulletin. Series 5. Geography* (6), pp.26-32 (in Russian with English summary).

Reistad M., Breivik O., Haakenstad H., Aarnes O. J., Furevik B. R., and Bidlot J. R. (2011). A high-resolution hindcast of wind and waves for the North Sea, the Norwegian Sea, and the Barents Sea. *Journal of Geophysical Research: Oceans*, 116(C5).

Rusu L., de León S., and Soares C. (2015). Numerical modeling of the North Atlantic storms affecting the West Iberian coast. *Maritime Technology and Engineering*, 978-1.

Saha S. et al. (2010). The NCEP climate forecast system reanalysis. *Bull. Am. Meteorol. Soc.*, 91(8), pp.1015-1057.

Saha S. et al. (2014). The NCEP Climate Forecast System Version 2. *J. Climate*. 27, pp. 2185-2208. DOI: 10.1175/JCLI-D-12-00823.1.

Soomere T. and Räämet A. (2014). Decadal changes in the Baltic Sea wave heights. *Journal of Marine Systems*, 129, pp. 86-95.

Soomere T., Behrens A., Tuomi L. and Nielsen J. (2008). Wave conditions in the Baltic Proper and in the Gulf of Finland during windstorm Gudrun. *Natural Hazards & Earth System Sci.*, 8(1), pp.37-46.

Stocker T. (Ed.). (2014). *Climate change 2013: the physical science basis: Working Group I contribution to the Fifth assessment report of the Intergovernmental Panel on Climate Change*. Cambridge University Press.

Stopa J., Arduin F., and Girard-Arduin F. (2016). Wave climate in the Arctic 1992-2014: seasonality and trends. *Cryosphere*, 10(4), pp.1605-1629.

Surkova G. (2015 October). Climate projection of storm weather patterns, In: Özhan, E. (Ed.). *Proceedings of the Twelfth International Conference on the Mediterranean Coastal Environment MEDCOAST 15*, Varna, Bulgaria, pp.531-540.

Surkova G., Arkhipkin V., and Kislov A. (2013). Atmospheric circulation and storm events in the Black Sea and Caspian Sea. *Central European Journal of Geosciences*, 5(4), pp.548-559. DOI : 10.2478/s13533-012-0150-7.

Surkova G. and Krylov A. (2017) Extremely Strong Winds And Weather Patterns // *Proceedings of the Thirteenth International Conference on the Mediterranean Coastal Environment MEDCOAST 17*. Turkey.

Taylor K. E., Stouffer R. J., and Meehl G. A. (2012). An overview of CMIP5 and the experiment design. *Bulletin of the American Meteorological Society*, 93(4), pp.485-498

Tolman H. L. (2009). User manual and system documentation of {WAVEWATCH-III} Version 3.14. US: Department of Commerce, National Oceanic and Atmospheric Administration, National Weather Service, National Centers for Environmental Prediction.

Wang X. L. and Swail V. R. (2001). Changes of extreme wave heights in Northern Hemisphere oceans and related atmospheric circulation regimes. *Journal of Climate*, 14(10), pp.2204-2221. DOI:10.1175/1520-0442(2001)014<2204:coewhi>2.0.co;2.

Zaitseva-Pärnaste I., Suursaar Ü., Kullas T., Lapimaa S., and Soomere T. (2009). Seasonal and long-term variations of wave conditions in the northern Baltic Sea. *J. Coast. Res.* SI(56) pp.277-281.



**Stanislav A. Myslenkov** is a Senior Researcher at the Department of Oceanology, Faculty of Geography, Lomonosov Moscow State University, Russia. He received the PhD in 2017. Research interests are wind waves, wave energy, ocean currents, experimental oceanography.